

# Serviceability limit state compressive strength for stiffened steel plates exhibiting column-like behavior

M. Rahman

*Bangladesh Bridge Authority, Dhaka 1212, Bangladesh*

Y. Okui & M.A. Anwer

*Saitama University, Saitama City, Saitama 338-8570, Japan*

**ABSTRACT:** Stiffened steel plates with high slenderness ratio parameters show large out-of-plane deflection under compression before reaching the ultimate buckling strength. While designing the slender stiffened plates, it is important to consider the serviceability limit state (SLS) compressive strength to avoid the large out-of-plane deflection. The SLS strength for wide stiffened plates (with low aspect ratio) exhibiting column-like behavior was investigated with nonlinear elasto-plastic finite element (FE) analysis, considering geometric and material nonlinearity. Furthermore, the probabilistic distribution of the SLS strengths was obtained by employing Monte Carlo simulations in association with the response surface method. Finally, the probabilistic SLS strengths were compared with the ultimate limit state (ULS) strength of different design codes i.e. JSHB, AASHTO, and Canadian Code where the SLS strength with the 5% probability of non-exceedance matches well with the ULS strength of JSHB, AASHTO, and Canadian Code.

## 1 INTRODUCTION

Due to high strength to weight ratio, stiffened steel plates are often used to construct different parts of steel bridges, such as the bottom flange of box girders, and the box sections used as truss members or columns. Under compression, such thin plate components exhibit local buckling and may fail with sudden collapse. The stability and buckling behavior of stiffened plates under compression is somewhat complicated because the resistance to compression is sensitive to a large number of parameters, such as the reduced slenderness parameter, the relative stiffness of stiffeners, the plate and stiffener geometry, and the boundary conditions.

Stiffened plates with high slenderness, i.e. width-to-thickness ratio parameter  $R_R > 1.0$ , shows large out-of-plane deflection due to elastic buckling. The parameter  $R_R$  is defined in the Japanese Specification for Highway Bridges (JSHB) (Japan Road Association, 2012) by

$$R_R = \frac{b}{t} \sqrt{\frac{\sigma_y}{E} \frac{12(1-\nu^2)}{\pi^2 k_r}} \quad (1)$$

Where  $b$  is the overall width of stiffened plate;  $t$  represents the thickness of stiffened plate;  $\sigma_y$ ,  $E$  and  $\nu$  represent the yield strength, modulus of elasticity, and Poisson's ratio of the steel, respectively, and buckling coefficient  $k_r = 4n^2$ , where  $n$  is the number of subpanels divided by the longitudinal stiffeners.

Kanai & Otsuka (1977) carried out experiments on 43 stiffened plates under uniaxial loading and reported that test specimens with  $R_R = 1.2$  yield large out-of-plane plastic deformation. Deformation of the plates occurs before they reach ultimate strength, at nearly half of the maximum load. As a consequence, Kanai and Otsuka recommended that out-of-plane deflection limit be of primary consideration in the design of slender stiffened plates, instead of ultimate strength.

According to ISO 2394 (1998), the SLS includes three different aspects among which unacceptable deformation is one. For compressive steel plates, criterion based on elastic buckling followed by unacceptable deformation is often considered for the SLS design (Paik & Thayamballi 2003). For example, checking the SLS related to out-of-plane deflection is necessary in the Nordic code (DNV 2002) for stiffened plates with a span-to-thickness ratio greater than 120. In a recent study (Rahman et al. 2018), the authors proposed the SLS compressive strength for stiffened plates based on elastic buckling and out-of-plane deflection restricting to a limit i.e. the fabrication tolerance.

Depending on the aspect ratio and the level of stiffening, stiffened plates may exhibit two distinct types of behavior: a plate-like behavior and a column-like behavior. Plate-like buckling refers to the global buckling of the entire panel along with the longitudinal stiffeners, where the stiffened plates possess a significant post-buckling strength reserve (Beg et al. 2012). However, wide stiffened plates with low aspect ratio ( $\alpha \leq 1.0$ ) exhibit column-like buckling that does not have any post-buckling strength reserve. Furthermore, Braun (2010) pointed out that, for column-like buckling, the sensitivity of initial geometric imperfection is higher than that of plate-like buckling.

Unlike ULS, the SLS for stiffened plates under compression is a relatively less frequently studied topic, despite its importance for efficient structural design. Moreover, due to the higher sensitivity of initial geometric imperfections on column-like buckling, investigating probabilistic SLS compressive strength such as a probability density function, a mean value, and a standard deviation is important rather than deterministic strength.

In this paper, the SLS compressive strength for wide stiffened plates exhibiting column-like behavior was investigated through nonlinear elasto-plastic finite element (FE) analysis, considering the variations in initial imperfections. The plates of normal steels, e.g. SM490Y and SM570 were considered, with thickness varied from 10 to 30 mm. Response surface functions were employed to estimate the variability of the strengths at SLS due to the variation of initial imperfections. After carrying out a total of 540 finite element analyses (FEAs) with varying parameters and obtaining response surfaces, the probabilistic distribution of compressive strengths at SLS was obtained through Monte Carlo simulation (MCS).

## 2 STIFFENED PLATE MODELS

### 2.1 Geometric Configuration

Longitudinally stiffened steel plates, as shown in Figure 1, with an aspect ratio ( $\alpha = a/b = 1$ ) and with three equidistant flat-type longitudinal stiffeners, satisfying the relative stiffness requirement of JSHB ( $\gamma_l/\gamma_{l,req} = 1$ ) were considered in the present study, which is supposed to produce the column-like buckling behavior. Here,  $a$  is the length of the plate, i.e., the distance between two transverse stiffeners,  $\gamma_l$  is the relative stiffness of the longitudinal stiffeners, and  $\gamma_{l,req}$  is the required relative stiffness to avoid whole-plate buckling.

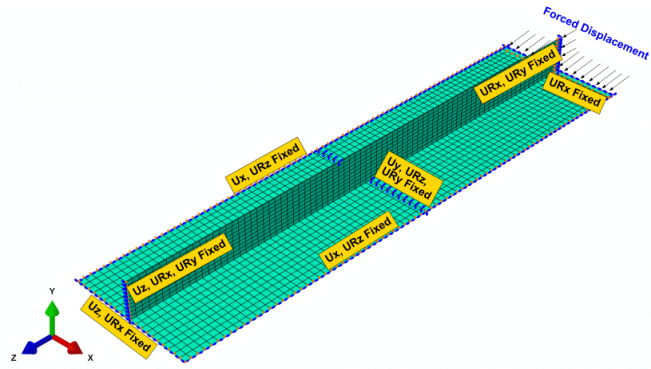
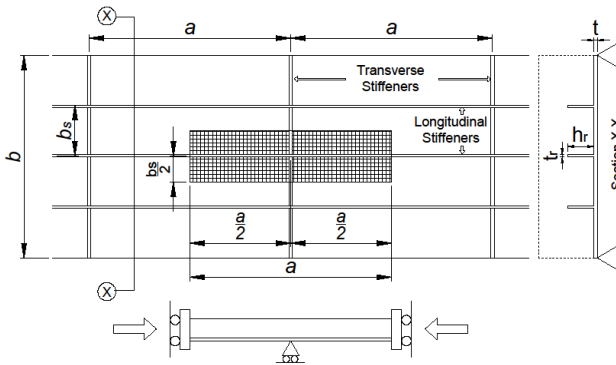


Figure 1. Stiffened plate model geometry.

Figure 2. Boundary conditions.

Table 1. Detailed dimensions of stiffened plate models.

$R_R$	$t$	$b$	$n$	$h_r$	$t_r$	$\gamma_l/\gamma_{l,req}$	$R_R$	$t$	$b$	$n$	$h_r$	$t_r$	$\gamma_l/\gamma_{l,req}$
SM490Y							SM570						
1.0	10	1780	4	95	11	1.04	1.0	10	1586	4	85	14	1.04
	30	5416	4	290	31	1.02		30	4810	4	280	31	1.02
	50	9292	4	490	50	1.01		50	8201	4	470	51	1.01
1.2	10	2136	4	100	11	1.03	1.2	10	1903	4	90	14	1.02
	30	6499	4	310	30	1.03		30	5772	4	290	33	1.02
	50							50	9841	4	490	53	1.01
1.4	10	2492	4	105	11	1.04	1.4	10	2220	4	95	14	1.07
	30	7582	4	320	31	1.02		30	6734	4	300	34	1.02

## 2.2 Material Model

The elastic properties, i.e. modulus of elasticity ( $E$ ) and Poisson's ratio ( $\nu$ ) were considered identical for SM490Y and SM570 steels and the values were taken as 200 GPa and 0.3, respectively. The inelastic characteristics of the two materials were determined from the idealized uniaxial stress ( $\sigma$ )-strain ( $\epsilon$ ) relationships obtained from test data (JSSC 2013) as presented in Table 2. Mises plasticity, the associated flow rule, and the isotropic strain hardening theory were applied to model the material nonlinearity in the nonlinear FE analysis.

Table 2. Inelastic characteristics of steel grades.

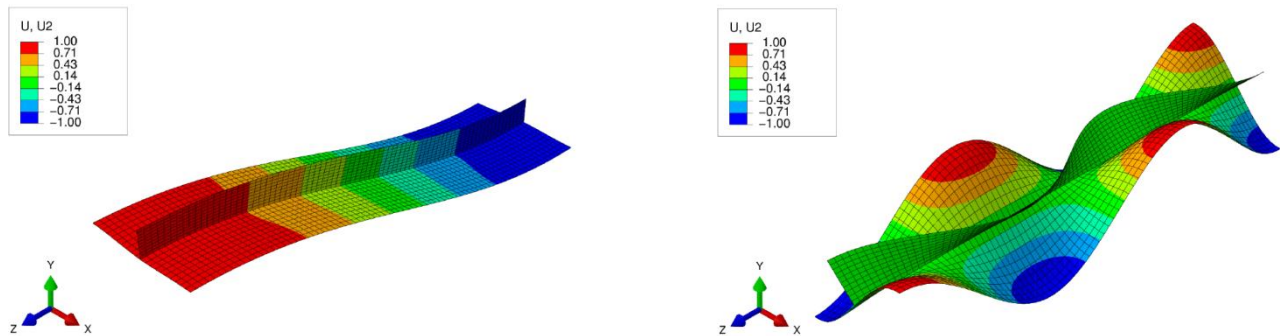
Sl. No.	SM490Y		SM570	
	$\epsilon/\epsilon_y$	$\sigma/\sigma_y$	$\epsilon/\epsilon_y$	$\sigma/\sigma_y$
1	1	1	1	1
2	10	1	3	1
3	23	1.14	15	1.12
4	50	1.28	32	1.17
5	100	1.28	50	1.17

## 3 DETERMINISTIC FINITE ELEMENT ANALYSIS (FEA)

To reduce the computational time, a part of the model (shaded rectangular area in Figure 1) was analyzed with ABAQUS. The plate members were modeled using 4-node, quadrilateral, stress-displacement shell element S4R, suitable for large displacement analysis. Considering the continuity of the plate along the longitudinal direction, removal of the effect of longitudinal edge support, and symmetric loading and boundary conditions, a strut model, as shown in Figure 2, was selected for numerical analysis. Here,  $U_x$ ,  $U_y$ ,  $U_z$  denote translational, and  $UR_x$ ,  $UR_y$ ,  $UR_z$  denote rotational degree of freedoms in X, Y and Z axis. Compressive load was applied through a forced displacement at the end of panel plate and the stiffener.

### 3.1 Eigenvalue Buckling Analysis

Eigenvalue buckling analyses were performed prior to nonlinear analyses to determine the elastic buckling strengths and buckling modes. In most of the cases, the first buckling mode was a local buckling mode. Two important buckling modes, i.e., the whole-plate mode and local mode are presented in Figures 3(a) and 3(b), respectively.



(a) (b)  
Figure 3. Elastic buckling modes (a) whole-plate mode, and (b) local mode.

### 3.2 Nonlinear Elasto-Plastic Analysis

Nonlinear elasto-plastic finite element analysis was carried out considering both geometric and material nonlinearity. As a source of variability of the compressive strengths, initial imperfections, i.e. whole-plate initial out-of-plane deflections, local initial out-of-plane deflections, and residual stresses were considered simultaneously. On the basis of respective mean values and standard deviations as shown in Table 3, 36 different combinations of imperfections were considered for a single stiffened plate model as presented in Table 4. In Table 3,  $\sigma_{rc}$  is the residual compressive stress,  $\delta_{0I}$  is the magnitude of whole-plate mode initial out-of-plane deflection,  $\Delta_{ini}$  is the magnitude of initial out-of-plane local deflection, and  $b_s$  is the width of a subpanel be-

tween two longitudinal stiffeners. The variables  $x_1$ ,  $x_2$ , and  $x_3$  represent the non-dimensional initial imperfections for residual stress, initial whole-plate out-of-plane deflections, and initial local out-of-plane deflections respectively (see Table 3). The nonlinear analysis was carried out in two steps. In the first step, initial imperfections were simulated to represent the initial condition, and, in the second step, compressive loading was applied through forced displacement. The initial out-of-plane deflections were simulated with buckling modes obtained from the elastic buckling analysis. Residual stresses were included directly in each element. A total of 540 FE analyses were carried out for 15 different plate models.

Table 3. Statistical parameters for initial imperfections obtained from previous studies (Nara & Komatsu 1988, Fukumoto & Itoh 1984, Komatsu et al. 1980).

Imperfections	Mean ( $\mu$ )	Standard deviation ( $\sigma$ )
$x_1 = \sigma_{rc}/\sigma_y$	0.230	0.145
$x_2 = 1000\delta_{01}/a$	0.096	0.426
$x_3 = 150 \Delta_{ini} /b_s$	0.138	0.107

Table 4. Initial imperfection combinations for a single stiffened plate model.

Sl. No.	$x_1 = \sigma_{rc}/\sigma_y$	$x_2 = 1000\delta_{01}/a$	$x_3 = 150 \Delta_{ini} /b_s$	Sl. No.	$x_1 = \sigma_{rc}/\sigma_y$	$x_2 = 1000\delta_{01}/a$	$x_3 = 150 \Delta_{ini} /b_s$
1	$\mu-\sigma$	$\mu$	0	19	$\mu+\sigma$	$\mu-2\sigma$	0
2	$\mu-\sigma$	$\mu$	$\mu+2\sigma$	20	$\mu+\sigma$	$\mu-2\sigma$	$\mu+2\sigma$
3	$\mu-\sigma$	$\mu$	$\mu+8\sigma$	21	$\mu+\sigma$	$\mu-2\sigma$	$\mu+8\sigma$
4	$\mu-\sigma$	$\mu+3\sigma$	0	22	$\mu+\sigma$	$\mu$	0
5	$\mu-\sigma$	$\mu+3\sigma$	$\mu+2\sigma$	23	$\mu+\sigma$	$\mu$	$\mu+2\sigma$
6	$\mu-\sigma$	$\mu+3\sigma$	$\mu+8\sigma$	24	$\mu+\sigma$	$\mu$	$\mu+8\sigma$
7	$\mu$	$\mu-\sigma$	0	25	$\mu+2\sigma$	$\mu$	0
8	$\mu$	$\mu-\sigma$	$\mu+2\sigma$	26	$\mu+2\sigma$	$\mu$	$\mu+2\sigma$
9	$\mu$	$\mu-\sigma$	$\mu+8\sigma$	27	$\mu+2\sigma$	$\mu$	$\mu+8\sigma$
10	$\mu$	$\mu$	0	28	$\mu+2\sigma$	$\mu+3\sigma$	0
11	$\mu$	$\mu$	$\mu+2\sigma$	29	$\mu+2\sigma$	$\mu+3\sigma$	$\mu+2\sigma$
12	$\mu$	$\mu$	$\mu+8\sigma$	30	$\mu+2\sigma$	$\mu+3\sigma$	$\mu+8\sigma$
13	$\mu$	$\mu+\sigma$	0	31	$\mu+3\sigma$	$\mu+\sigma$	0
14	$\mu$	$\mu+\sigma$	$\mu+2\sigma$	32	$\mu+3\sigma$	$\mu+\sigma$	$\mu+2\sigma$
15	$\mu$	$\mu+\sigma$	$\mu+8\sigma$	33	$\mu+3\sigma$	$\mu+\sigma$	$\mu+8\sigma$
16	$\mu$	$\mu+2\sigma$	0	34	$\mu+3\sigma$	$\mu+3\sigma$	0
17	$\mu$	$\mu+2\sigma$	$\mu+2\sigma$	35	$\mu+3\sigma$	$\mu+3\sigma$	$\mu+2\sigma$
18	$\mu$	$\mu+2\sigma$	$\mu+8\sigma$	36	$\mu+3\sigma$	$\mu+3\sigma$	$\mu+8\sigma$

## 4 FEA RESULTS AND RESPONSE SURFACE FOR SLS

### 4.1 The SLS and Its Determination Criteria

The fabrication tolerance is often used as a limiting criterion for excessive out-of-plane deflection. Nara & Komatsu (1988) reported the fabrication tolerance in the JSHB. The fabrication tolerance for whole-plate out-of-plane deflection shape is  $\delta \leq a/1000$ , and for local out-of-plane deflection shape is  $\Delta \leq b_s/150$ , where  $\delta$  and  $\Delta$  are the highest out-of-plane deflection magnitude after loading for the whole-plate and the local deflection shape, respectively.

In this research, the compressive strength at SLS ( $\sigma_{SLS}$ ) was defined in the elastic range (e.g., plasticity does not occur), as the strength corresponding to the fabrication tolerance, as follows:

$$\sigma_{SLS} = \begin{cases} \text{for whole-plate deflection, } \sigma \text{ at } \delta = \frac{1000}{a} \\ \text{for local deflection, } \sigma \text{ at } \Delta = \frac{150}{b_s} \end{cases} \quad (2)$$

Where,  $\sigma$  represents the corresponding stresses at fabrication tolerance. After checking the onset of plasticity,  $\sigma_{SLS}$  was confirmed to remain within the elastic range. Figure 4 describes the determination of compressive strengths at SLS from normalized stress versus out-of-plane deflection curves, as an example. In these figure, the fabrication tolerance is indicated by a vertical line. The SLS strength is the stress value corresponding to the intersection point between the vertical line and the normalized stress versus out-of-plane deflection curve. The initiation of plasticity occurred between  $\sigma_{SLS}$  and  $\sigma_{ULS}$ .

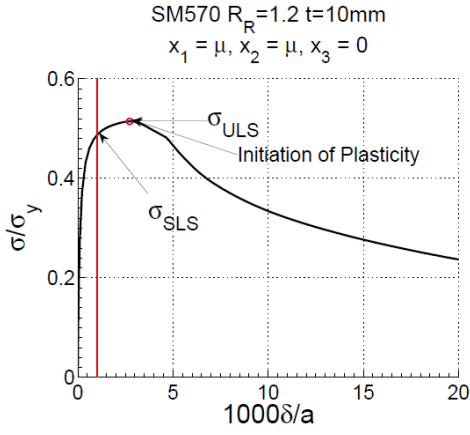


Figure 4. Normalized stress versus out-of-plane deflection curves.

#### 4.2 Response Surface for SLS

After determining the  $\sigma_{SLS}$ , the response of the  $\sigma_{SLS}$  due to the variations in initial imperfections, material grade, and the plate thickness is investigated for stiffened plates using the response surface function as described in Equation 3.

$$\frac{\sigma_{SLS}}{\sigma_y} = \sum p_{ijk} x_1^i x_2^j x_3^k; \quad (i = 0 \sim 2; j = 0, 2; k = 0, 2; i + j + k \leq 6) \quad (3)$$

Where  $\sigma_y$  is the yield strength,  $p_{ijk}$  are the coefficients of the polynomial, as determined by a nonlinear multiple regression analysis. The sample dataset of the regression analysis at a certain  $R_R$  includes the  $\sigma_{SLS}$  data for all of the material grades and all of the thickness variations. Since the response surface function comprises three variables (i.e.  $x_1$ ,  $x_2$ , and  $x_3$ ), the response of  $\sigma_{SLS}$  is presented in Figure 5 with respect to two variables while the third variable is maintained constant. In this figure, the mesh grid represents the response surface and the circular dots indicate the  $\sigma_{SLS}$  values obtained from the FEA.

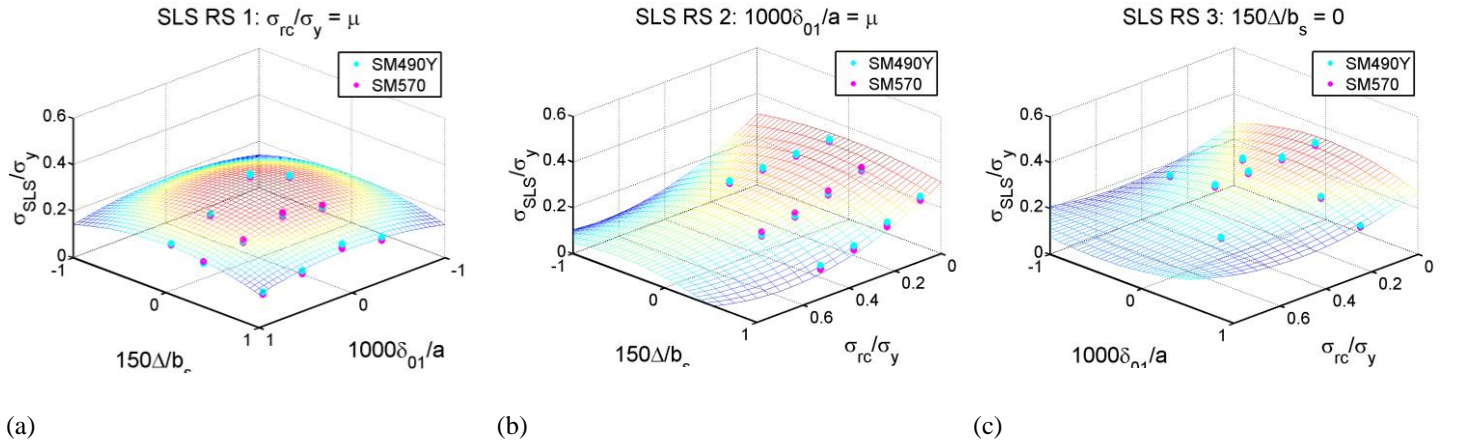


Figure 5. Response surfaces (RS) for  $\sigma_{SLS}$  at  $R_R = 1.4$ . (a) RS 1: variation of  $x_2$  and  $x_3$  for the case in which  $x_1 = \mu$ ; (b) RS 2: variation of  $x_1$  and  $x_3$  for the case in which  $x_2 = \mu$ , and (c) RS 3: variation of  $x_1$  and  $x_2$  for the case in which  $x_3 = 0$ .

## 5 PROBABILISTIC ANALYSIS

Using the response surfaces, Monte Carlo simulations (MCS) were carried out in order to obtain probabilistic information of compressive strengths at different  $R_R$  values. In the MCS,  $x_1$ ,  $x_2$ , and  $x_3$  were considered to be three independent random variables. In the first realization, one set of random values for  $x_1$ ,  $x_2$ , and  $x_3$  were generated in accordance with their respective probability density functions (PDFs), as reported in previous studies (Nara & Komatsu 1988, Fukumoto & Itoh 1984, Komatsu et al. 1980). The set of random values was then placed in the response surface function (Eq. 3) in order to determine the normalized compressive strength SLS ( $\sigma_{SLS}/\sigma_y$ ), for that set of initial imperfections. The realizations continued until the convergence of the MCS result, i.e., until the mean value and standard deviation of  $\sigma_{SLS}/\sigma_y$  obtained from several realizations, become convergent. A total of 100,000 realizations were required in order to obtain a convergent MCS result.

After performing MCS for each value of  $R_R$ , the relative frequency distributions of  $\sigma_{SLS}/\sigma_y$  were plotted. Figure 6(a) and 6(b) shows the relative frequency distributions for  $\sigma_{SLS}/\sigma_y$  at  $R_R = 1.0$  and 1.4 respectively.

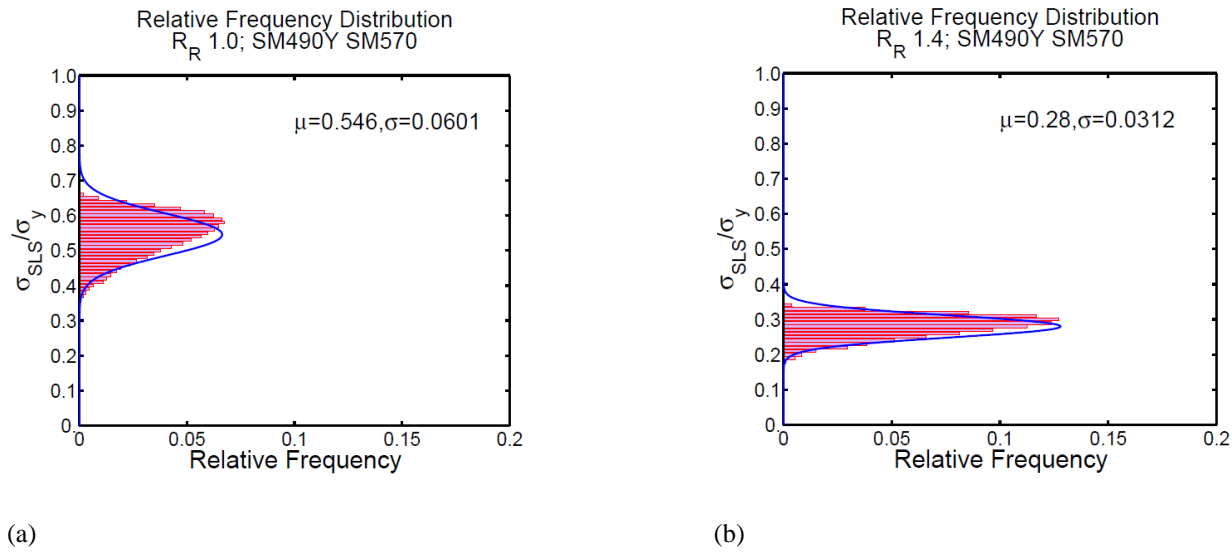


Figure 6. Relative frequency distribution for normalized compressive strength at SLS ( $\sigma_{SLS}/\sigma_y$ ) at (a)  $R_R = 1.0$ , and (b)  $R_R = 1.4$ .

## 6 RESULT AND DISCUSSION

Summary of the MCS result is presented by the blue color error bars in Figure 7. Here, the middle circles represent the mean values of normalized compressive strengths at SLS while the upper and lower error bars depicts the probability of non-exceedance ( $p_f$ ) 5% and 95% respectively. The probabilistic SLS strengths are compared with the probabilistic ULS strengths of the same stiffened plate model reported by the authors elsewhere (Rahman et al., in press). Moreover, the ULS strengths obtained from different design codes e.g. JSHB, AASHTO, and Canadian Code are also compared with the current study result.

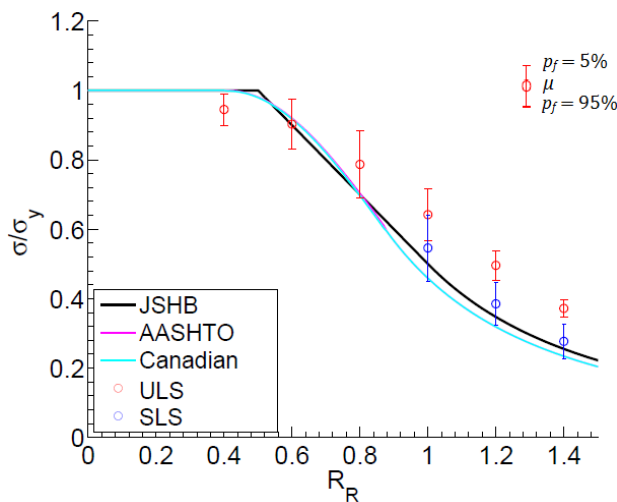


Figure 7. Comparison of MCS result for  $\sigma_{SLS}$  with ULS strengths from Rahman et al. (2020), JSHB, AASHTO, Canadian Code.

From the Figure 7, it is evident that the AASHTO and Canadian Code provide identical ULS strength results, which agree well with the JSHB. The mean values of the normalized SLS strengths, obtained from this study, are slightly higher than the JSHB ULS strengths. However, in comparison with the mean values of normalized ULS strengths reported by the authors, the mean values of the normalized SLS strengths are 18%, 29%, and 34% lower at  $R_R$  values 1.0, 1.2, and 1.4 respectively. Interestingly, the coefficient of variation of SLS strengths is higher than that of the ULS strengths.

Current study provides the probabilistic information of SLS compressive strengths of stiffened steel plates, which can be used as an important baseline for developing reliability based design strength curve.

## REFERENCES

- Beg, D., Kuhlmann, U., Davaine, L., & Braun, B. 2012. *Design of Plated Structures: Eurocode 3: Design of Steel Structures, Part 1-5 - Design of Plated Structures*: First Edition, ECCS, Berlin, Germany.
- Braun, B. T., 2010. *Stability of steel plates under combined loading*, Doctoral dissertation Institut für Konstruktion und Entwurf; Universität Stuttgart, Germany.
- Det Norske Veritas (DNV). 2002. Buckling strength of plated structures, *Recommended Practice DNV-RP-C201*, Norway.
- Fukamoto, Y. & Itoh, Y. 1984. Basic compressive strength of steel plates from test data. *Proc. of Structural Eng./Earthquake Eng., JSCE*, 344(I-1), 129-139.
- ISO 2394. 1998. *General principles on reliability for structures*, International Organization for Standardization, Geneva, Switzerland.
- JSHB 2012. *Specification for Highway Bridges Part-II Steel bridges*. Japan Road Association
- JSSC report 2013. *Rationalization of strength design for steel bridges, Technical report No. 98*, Research committee for rational structure and design for steel bridges, Japan Society of Steel Construction (JSSC). (In Japanese)
- Kanai, M. & Otsuka K. 1977. Design method of stiffened plate. *Civil Engineering Journal*. 19(10): 498-503. (In Japanese)
- Komatsu, S., Kitada, T., Watanabe, E., Akiraumi, M., & Nara, K. 1980. Statistical study of the initial deformation and the ultimate strengths of steel bridge members, *JSSC*, 16, 10-43. (In Japanese)
- Nara, S. & Komatsu, S. 1988. Statistical study on ultimate strength curves of longitudinally stiffened plates under uniaxial compression. *Journal of Structural Mechanics and Earthquake Engineering*, 392(I-9), 289-296. (In Japanese)
- Paik, J. K. & Thayamballi, A. K. 2003. *Ultimate limit state design of steel plated structures*. West Sussex: Wiley publications.
- Rahman, M., Okui, Y., and Anwer, M.A. 2018. Probabilistic strength at serviceability limit state for normal and SBHS slender stiffened plates under uniaxial compression. *International Journal of Steel Structures* 18: 1397–1409
- Rahman, M., Okui, Y., Komuro, M., Anwer, M. A., and Numata, A., In Press: Probabilistic compressive strength of stiffened steel plates exhibiting column-like behavior: ultimate and serviceability limit states, *ASCE Journal of Structural Engineering*, DOI: 10.1061/(ASCE)ST.1943-541X.0002719.